Effect of plasma ion implantation on the hydrogen embrittlement of Cu strengthened HSLA-100 steel

A. KUMAR, S. TARAFDER
National Metallurgical Laboratory, Jamshedpur 831007, India
S. MUKHERJEE
FCIPT, Institute for Plasma Research, Gandhinagar 382044, India
S. K. DAS, B. RAVIKUMAR, I. CHATTORAJ*
National Metallurgical Laboratory, Jamshedpur 831007, India
E-mail: ichatt_62@yahoo.com

The effect of low dosage plasma ion implantation on hydrogen embrittlement was studied for an HSLA steel using notched tensile samples. The plasma treatment caused an enhancement in the linear strain to failure under embrittling conditions. This was however not reflected in the fracture surfaces of the treated samples which had similar fractographic features as those of untreated samples. The plasma treatment delayed the process of embrittlement without causing any alteration in the basic mechanism of embrittlement. This was due to introduction of residual compressive stresses as well as reduction in the hydrogen permeation flux. Implantation in pure nitrogen seemed most beneficial while implantation in pure argon caused very little improvement.

1. Introduction

Surface modification techniques are convenient means to reduce hydrogen embrittlement as they preserve the bulk properties while changing the surface resistance to hydrogen absorption, sub-surface hydrogen diffusion and cracking propensity. Ion implantation as a surface modification tool to counter hydrogen embrittlement seems attractive as it causes changes in the surface chemistry, introduces surface compressive stresses that retard cracking, and impregnates elements that may act as interstitial diffusion barriers. The shortcomings of conventional ion implantation are overcome by plasma source ion implantation (PSII) and plasma immersion ion implantation (PIII) where target manipulation is not required since the plasma completely surrounds the target. The PSII process [1, 2] provides means of circumventing the line of sight restrictions of conventional ion implantation. These methods allow homogenous distribution of the implanted species and treatment of complex shapes.

While ion implantation is a popular tool in tribology related problems, it has been used only sparingly as a means to reduce or counter hydrogen embrittlement. This was partly due to the non-availability of the aforementioned processes capable of uniform implantation and implantation of complex shapes. Plasma processes have been used for reducing hydrogen entry and embrittlement [3–9]. However, most of these works concentrated on the use of plasma methods to reduce hydrogen permeation [4–9]. Moreover, they used nitriding or carbonitriding processes [4, 6–8], which have a much higher intrusion depth (hundreds of microns) as compared to PSII (few microns). Plasma nitriding and carbonitriding result in significant amounts of brittle iron nitride phases, they also require elevation of the substrate temperature which may cause undesirable microstructural alterations. There is no report on the utilisation of PSII to counter hydrogen embrittlement; needless to say PSII introduces much lower amounts of detrimental nitrides and it can be a near-ambient process. This article reports our initial findings on the effects of low dose plasma implantation on the hydrogen embrittlement of a high strength steel.

2. Experimental procedures

The material used as the substrate in this study was a Cu-strengthened HSLA-100 steel with the composition (in weight %):C-0.05, Mn-1.0, S-0.001, Si-0.34, Cu-1.23, Ni-1.77, Cr-0.61, Mo-0.51, Al-0.025, Nb-0.037, P-0.009, Fe-balance. It was obtained in the form of quenched and tempered rolled plates of 2” (50 mm) thickness. The steel had an acicular ferrite microstructure, a tensile strength of 740 MPa, an uniaxial yield

*Author to whom all correspondence should be addressed.

0022–2461

strength (σ_{ys}) of 650 MPa, and a hardness of 280VPN. Coupons and tensile samples were fabricated from the plates without any further treatment.

The coupons for permeation studies were machined to dimensions of 0.5 mm × 40 mm × 40 mm, with the thickness direction perpendicular to the rolling direction. The coupon surfaces were polished with 1200-grit emery paper. Axisymmetric notched tensile samples with a gauge diameter of 8 mm ($\mp$0.01 mm) and a total gauge length of 50 mm were fabricated with the gauge length parallel to the rolling direction. The notch was machined in the middle of the gauge section with a notch tip radius (ρ) of 0.5 mm ($\mp$0.02 mm). The coupons as well as tensile samples were ion implanted using the PSII technique as follows. The samples were placed on a conducting sample holder that was biased pulsed negative to voltages of 1 kV, with the pulse on time of 50 μs at a repetition rate of 1 KHz. The average current density during implantation was 10 mA cm^{-2}. The implantation was done for 3 h with the chamber maintained at 10^{-3} mbar pressure. The substrate temperature was not allowed to exceed 100°C. Two different gas mixtures were used for the plasma, a Nitrogen-Hydrogen (N—H) mixture and an Argon–Nitrogen (Ar—N) mixture. Three sets of gas ratios were used in each mixture, corresponding to 100%, 75% and 25% of the first named gas in each mixture. This produced six different plasma treatment conditions. More details about the experimental set-up have been described elsewhere [10–12]

Permeation and slow strain rate testing were conducted in 0.1 N NaOH solution, at ambient temperature (300 K). Permeation experiments were conducted using the double cell method [13]. Cathodic charging current densities (I_c) of 0.5 mA cm^{-2} and 10 mA cm^{-2} were used during *in-situ* hydrogenation of tensile samples, representing two different severities of embrittling environment. The notched tensile specimens were subjected to slow strain rate loading under displacement control mode, with *in-situ* hydrogen charging done in a Perspex cell attached to the loading assembly. The hydrogen charging was initiated simultaneously with the slow strain rate loading. A displacement rate of 5×10^{-4} mm s^{-1} was used for the embrittlement experiments, which corresponded to a nominal global strain rate of 1×10^{-5} s^{-1}.

The residual stress measurements were done using an X-ray stress analyser that determines residual stresses through peak shift measurements. Components of the residual stress are reported corresponding to the length and breadth direction of the implanted coupons. The choice of this representation is arbitrary and merely represents two mutually orthogonal directions. Fracture surfaces were observed under a scanning electron microscope.

3. Results and discussions

The stress-strain curve for the notch tensile specimens with different implantation are shown in Figs 1 and 2. Stress values were calculated using the original notch dimensions, the strains were calculated from the measured linear extensions. It needs to be mentioned that the notch root strain is much more complex and requires a radial strain gauge to measure it. The latter is not feasible for our experiments as the sample cracks at the notch tip, moreover, the presence of an aqueous environment prohibits the use of a gauge. Fig. 1 shows the behaviour of samples implanted in a N_2—H_2 mixture, Fig. 2 is for samples implanted in an Ar—N_2 mixture. The behaviour of an untreated sample exposed to the more severe environment (that is one which is hydrogen charged at 10 mA cm^{-2}) is also included. These steels have low work hardening capacity which is apparent from the long plateau present for the base steel specimen tested in air. The stress-strain curves indicate a gradual rupture instead of an abrupt rupture. This is due to the fact that the final failure is by ductile mechanisms and is very similar to overload failure.

It may be observed that even after implantation, the material has much less ductility in hydrogen charging situations as compared to its failure in air. The

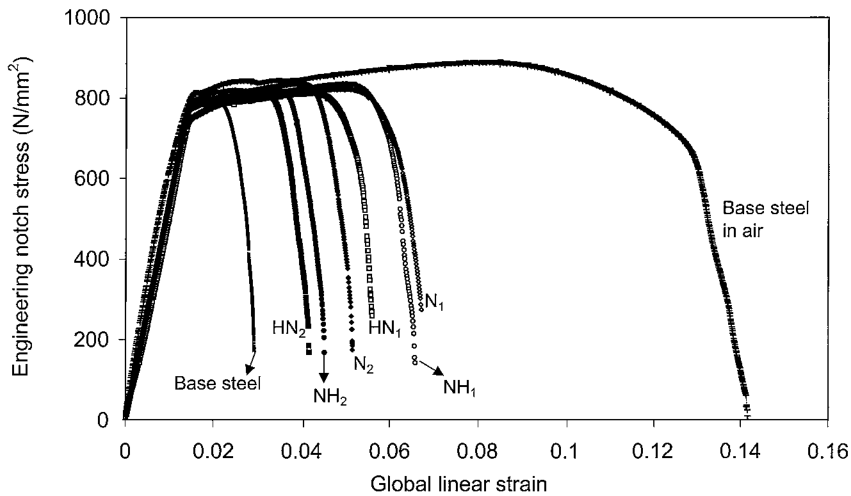

Figure 1 Stress-strain curves in embrittling conditions for N_2—H_2 implanted notched tensile specimens. N, NH and HN correspond to treatments done in pure N, 75% N and 25% N respectively while the subscripts 1 and 2 indicate the two embrittling conditions with charging current densities $I_c = 0.5$ mA/cm^2 and $I_c = 10$ mA/cm^2 respectively. Curves for untreated base steel tested in air and tested under the more severe hydrogen charging condition ($I_c = 10$ mA/cm^2) are included.

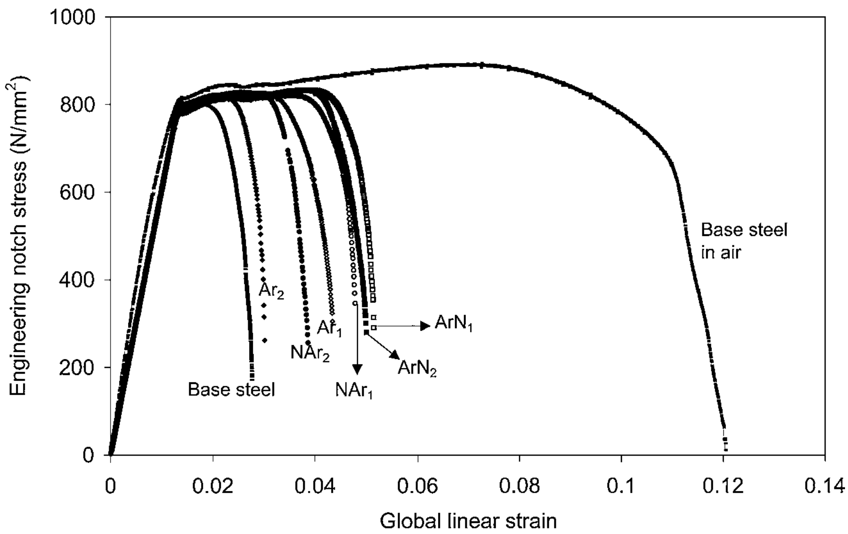

Figure 2 Stress-strain curves in embrittling conditions for Ar—N_2 implanted notched tensile specimens. Ar, ArN and NAr correspond to treatments done in pure Ar, 75% Ar and 25% Ar respectively while the subscripts 1 and 2 indicate the two embrittling conditions $I_c = 0.5$ mA/cm^2 and $I_c = 10$ mA/cm^2 respectively.

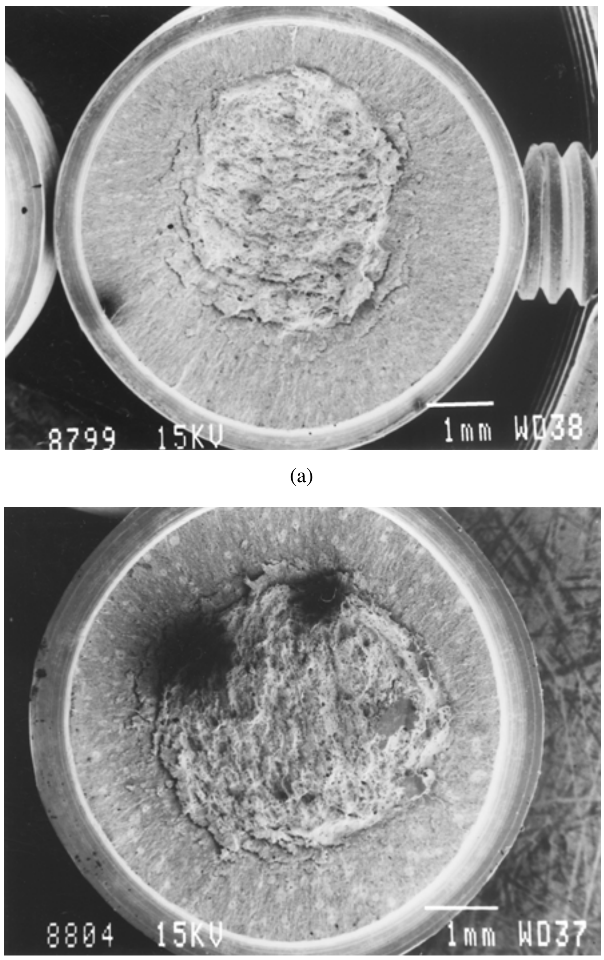

(a)

(b)

Figure 3 Fracture surface of untreated base steel exposed to the embrittling condition (a) $I_c = 10$ mA/cm^2 and (b) $I_c = 0.5$ mA/cm^2.

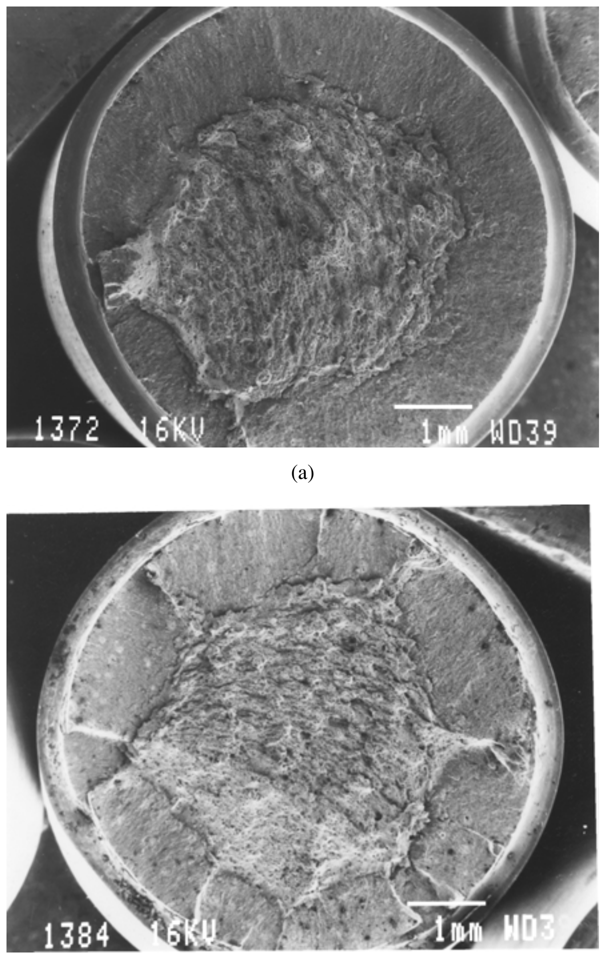

(a)

(b)

Figure 4 Fracture surface of steel sample ion implanted using pure nitrogen exposed to the embrittling condition (a) $I_c = 10$ mA/cm^2 and (b) $I_c = 0.5$ mA/cm.

fractographs for the base steel samples after embrittlement in the two conditions stated above are shown in Fig. 3. It may be noted that the fractographs show outer annular brittle regions that have quasi-cleavage fracture morphology and central dimpled ductile cores. The radial extent of the brittle region is greater in the higher severity environment. In spite of the much higher linear extension prior to fracture for the implanted samples, their fractographic features are not significantly different from that of the untreated steel sample. The fractographs for the treated samples are shown in Figs 4 and 5 corresponding to samples treated with two different

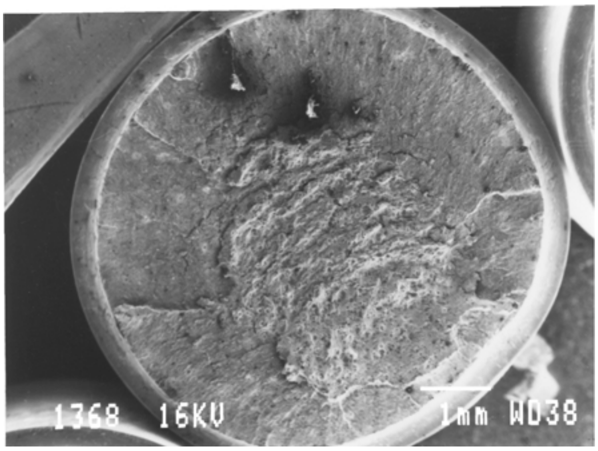

(a)

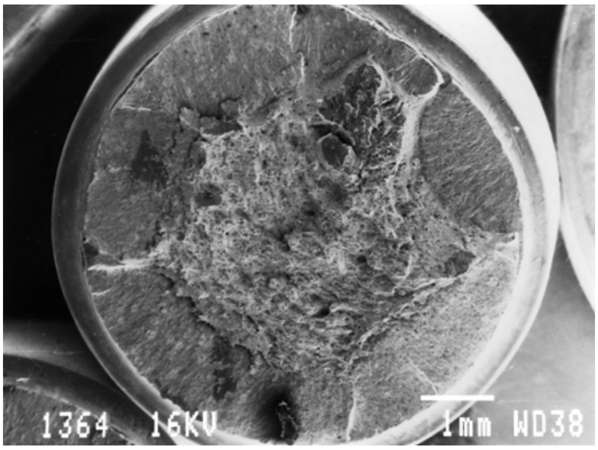

(b)

Figure 5 Fracture surface of steel sample ion implanted using nitrogen—hydrogen mixture (N_2:H_2 = 1:3) exposed to the embrittling condition (a) $I_c = 10$ mA/cm^2 and (b) $I_c = 0.5$ mA/cm^2.

N_2—H_2 mixtures. Higher magnification observation did not reveal any significant differences in the dimple sizes nor their distribution between the different samples. The difference in the lower severity samples (Figs 3b, 4b and 5b) was that the plasma treated samples had a number of thumbnail type brittle regions emanating from the surface and joined by radial ductile ligaments. This feature is much less evident but present even for plasma treated samples embrittled in the higher severity environment (Figs 4a and 5a). The thumbnails represent different crack planes, which are close to the notch plane but not coplanar, unlike the brittle crack fronts in the base steel samples. This is indicative of a cracking process that initiated at multiple sites instead of a single supercritical crack precursor. The increase in global strain to failure is also borne out by the reduction in the gauge diameter for the treated specimens as shown in Table I. The table also provides the relative extent of the brittle region for differently treated specimens and there is only marginal difference in the values as compared to base steel.

The overall effect of plasma treatment seems to be one of delaying the cracking rather than preventing it and this leads to higher failure strains (linear as well as radial). There are three possible reasons for the enhancement of failure strains. The first is a reduction in the amount of hydrogen ingress. The second possibility is blunting of incipient surface cracks (crack pre-cursors) due to elemental deposition during plasma treatment. The third is the possibility of introduction of surface compressive stresses that would delay crack initiation. We have observed that nitrogen implantation does lead to perceptible decrease in the hydrogen permeation, this effect is most when the implantation was carried out in pure nitrogen as shown in Table II. The hydrogen diffusion during slow straining occurs due to a concentration gradient imposed by the cathodic charging as well as the dynamic hydrostatic stress gradient across the specimen section. Thus an alteration of the surface electrochemistry or of the internal residual stress profile will interfere with the hydrogen diffusion. Moreover, occupation of the interstitial lattice sites will also retard hydrogen mobility by reducing the sites for hydrogen diffusion.

The induced residual stresses are shown in Table III. It may be noted that controlled polishing introduces compressive (negative) stresses in the untreated coupons. Plasma treatment causes enhancement of the compressive residual stresses in all cases except for treatment in a pure argon. The reduction in hydrogen permeation flux may partly be due to the induced compressive stress since hydrogen flux is retarded by a negative hydrostatic stress. The added presence of implanted

TABLE I Features of fracture surface after embrittlement in the more severe ($I_c = 10$ mA/cm^2) environment

Treatment condition—Gas ratio in plasma mixture	Reduction in gauge diameter (%)	Radial fraction of brittle zone
Base steel (no treatment)	3.92	0.488
Ar:N_2 = 1:3	5.38	0.422
Ar:N_2 = 3:1	6.21	0.387
Pure Ar	4.49	0.49
N_2:H_2 = 3:1	5.75	0.448
N_2:H_2 = 1:3	5.63	0.523
Pure N	6.38	0.379

TABLE II Hydrogen flux at an impressed charging current density of 1 mA/cm^2

Treatment condition—Gas ratio in plasma mixture	Steady state hydrogen permeation flux (μA/cm^2)
Untreated	2.73
Pure N_2	1.78
N_2:H_2 = 3:1	1.8
N_2:H_2 = 1:3	2.65

TABLE III Residual stresses in treated samples

Treatment condition—Gas ratio in plasma mixture	Residual stress (MPa)*	
	Length direction	Breadth direction
Base steel (no treatment)	−265	−275
Ar:N_2 = 1:3	−417	−318
Ar	−377	−275
Ar:N_2 = 3:1	−280	−407
N_2:H_2 = 3:1	−284	−441
N_2:H_2 = 1:3	−436	−291

*Negative values denote compressive stresses.

elements at the interstitial sites causes hindrance to hydrogen transport when the latter is by volume diffusion, this effect would be most, the higher the amount of implanted interstitial elements. It may be noted that the steady state permeation was not significantly decreased by the treatment N:H = 1:3. In this case the significant improvement in embrittlement resistance borne out by the reduction in area can be attributed to the considerable compressive stresses introduced by this treatment. Thus the compressive residual stress is able to delay crack initiation. This finding also seems to indicate that the presence of implanted nitrogen has a much more important role in reducing hydrogen permeation (for treatments N:H = 3:1 and pure Nitrogen) than does induced compressive stresses.

The enhancement of failure strains is however not reflected in the fracture morphology where the percentage of brittle failure remains relatively unaffected by the plasma treatments. The observations indicate a delay in the onset of the hydrogen embrittlement mechanism rather than a phenomenological change. Such a delay would be consistent with the presence of surface compressive stresses. In such a case, higher strains would be required (to offset the compressive stress) to attain the threshold stress for cracking. The observation of multiple (non-coplanar) cracks is indicative of this delay in crack initiation since statistically the higher the strains required for crack initiation, the higher the chance of a number of cracks initiating simultaneously. We attribute the lack of change in the percentage brittle fracture area when the elongation changed considerably to the fact that the crack propagation mechanism beyond the initial plasma implanted region would be similar to that of untreated base steel. The plasma implantation delays crack initiation but does not prevent it and once the crack grows beyond the plasma implanted subsurface, its kinetics of growth and the resultant fracture surface is similar to that of an untreated steel matrix. It should be appreciated that the brittle area in treated samples have similar area fractions as that of untreated samples but the cross section area is much reduced due to later onset of brittle cracking.

The possibility of a brittle nitride phase at the surface cannot be ruled out and is under investigation. The benefits in terms of reduction in hydrogen flux and higher compressive stresses may be partly annulled by a brittle superficial phase. In ion nitriding such a brittle phase is indeed responsible for the reduction in hydrogen flux [4]. This might explain the brittle microstructure in implanted samples in spite of the higher failure strains. Treatment in pure argon is not beneficial. But with nitrogen addition there is definite improvement in terms of the global strain to failure. For the treatments done in N_2—H_2 mixtures, pure nitrogen seems to be most beneficial with the benefits decreasing as the hydrogen amount in the mixture increases. This is possibly due to higher nitrogen retained in the subsurface. The possibility of residual hydrogen retained from the mixture and thus decreasing failure strain is not an issue, as hydrogen is not known to be impregnated during implantation. The nitrogen is also beneficial when used in an Ar—N_2 mixture, although there is no monotonic trend of improvement in this combination and it is harder to explain.

4. Conclusion

Higher linear strains to failure were observed in plasma treated samples (except when treated in pure Ar) as compared to untreated steel (HSLA) samples. Enhancement of residual compressive stress as well as a decrease in the hydrogen permeation flux, brought about by plasma treatment, have been observed. These are likely reasons for the enhancement of failure strains. The fracture surfaces however did not show much difference in terms of the fractional area of brittle zone. The plasma treatment delays the process of embrittlement without causing any alteration in the basic mechanism of embrittlement. The difference between different implanted samples was most likely due to different amounts of implanted species. Implantation in pure nitrogen seemed most beneficial while implantation in pure argon caused very little improvement. The possibility of a superficial brittle nitride phase is under investigation, this may counteract the accrued benefits of residual stress and reduced hydrogen diffusion.

Acknowledgements

This work is supported by a Grant-in aid from the Department of Science and Technology, Government of India.

References

1. F. J. WORZALA, J. R. CONRAD, R. A. DODD, M. B. MADAPURA and K. SRIDHARAN, in Proceedings of the 7th International Conference on Ion & Plasma Assisted Techniques ([IPAT 89], Geneva, Switzerland, 1989), p. 139.
2. K. SRIDHARAN, J. R. CONRAD, R. A. DODD and F. J. WORZALA, *Scripta Metall. Mater.* **26** (1992) 1037.
3. W. ENSINGER, *Surface & Coatings Tech.* **84** (1996) 434.
4. P. BRUZZONI, S. P. BRUHL, J. A. GOMEZ, L. NOSEI, M. ORTIZ and J. N. FEUGEAS, *ibid.* **110** (1998) 13.
5. A. M. BRASS, J. CHENE and A. BOUTRY-FOURVEILLE, *Corros. Sci.* **39** (1997) 1469.
6. A. H. BOTT, S. P. BRUHL, B. GOMEZ, M. A. ZAMPRONIO, P. E. V. MIRANDA and J. N. FEUGEAS, *J. Phys. D., Appl. Phys.* **31** (1998) 3469.
7. T. ZAKROCZYMSKI, N. LUKOMSKI and J. FLIS, *Metall. Foundry Engr.* **23** (1997) 147.
8. M. A. ZAMPRONIO, O. BARTIER, J. LESAGE and P. E. V. MIRANDA, *Mater. Manuf. Process* **10** (1995) 315.
9. T. ZAKROCZYMSKI, N. LUKOMSKI and J. FLIS, *Corros. Sci.* **37** (1995) 811.
10. S. MUKHERJEE and P. I. JOHN, *Surf. & Coatings Tech.* **93** (1997) 188.
11. Idem., *ibid.* **98** (1998) 1437.
12. S. MUKHERJEE, J. CHAKRABORTY, S. GUPTA, P. M. RAOLE, P. I. JOHN, K. R. M. RAO and I. MANNA, *ibid.* **156** (2002) 103.
13. M. DEVANATHAN and Z. STACHURSKI, *Proc. Royal Soc.* **A270** (1962) 90.

Received 22 July 2002
and accepted 3 April 2003